SUPPLEMENTARY INFORMATION

Development of efavirenz base model

The initial base model used *in vivo* CL_{po} (= 9.07 L/h; 26% CV) from multiple dose administration (unpublished data provided by BMS) as the clearance input. Volume of distribution (V_{ss}) was estimated from clinical data because of the uncertainty in efavirenz fu_p and logP and the high sensitivity of the predicted V_{ss} to these parameters.[1] First, a global tissue-to-plasma partition coefficient (K_p) scalar (minimal PBPK model) was fitted in order to recover the observed steady-state mean concentration-time profiles following the administration of 600 mg daily for 7 days (unpublished data provided by BMS) giving an estimated V_{ss} of 2.26 L/kg (Kp scalar = 0.155). All optimization was done using the Weighted Least Square algorithm and Nelder-Mead method.

The induction data were generated using cryopreserved human hepatocytes (Life Technologies Hu1206, Hu1191, Hu1198, Hu4193) as described previously.[2, 3] In brief, hepatocytes were incubated with varying concentrations of efavirenz prior to assessment of activity (6β-hydroxytestosterone and hydroxybupropion) and mRNA levels (QuantiGene Plex 2.0 Affymettrix Assay Kit). The CYP3A4 induction parameters selected for the model were based on mRNA levels (the activity data showed comparable Ind_{max}:$IndC_{50}$ ratio) [2] and were calibrated against rifampin data using the default Ind_{max} and $IndC_{50}$ for rifampin *in vivo* of 16-fold and 0.32µM, respectively. [2] For CYP2B6, induction parameters based on activity levels [4] were used without calibration in the final model. Although mRNA data were also generated, mRNA data showed systematically lower Ind_{max}:$IndC_{50}$ ratios compared to activity data and were generally more variable across several inducers.

The differential equations describing substrate kinetics using the minimal PBPK model, as well as dynamic enzyme inhibition/inactivation and induction have been published elsewhere. [5, 6]

The default enzyme turnover rate constants (kdeg) of 0.0217 hr^{-1} for CYP2B6, and 0.0193 hr^{-1} and 0.03 hr^{-1} for hepatic and intestinal CYP3A4, respectively, were used in all simulations.

Evaluation and refinement of CYP3A4 induction in the liver and gut: prediction of the effect of efavirenz 600 mg QD on alfentanil i.v. and p.o. pharmacokinetics

Ten virtual trials of 12 subjects (age 18-29 years, female prop. 0.5) receiving a single oral dose of alfentanil (15 µg/kg IV bolus in the morning of day 16, or 43 µg/kg p.o. in the morning of day 15), in the presence and absence of efavirenz treatment (600 mg QD given orally at bedtime for a total of 20 doses), were generated and the predicted and observed plasma concentration-time profiles and PK parameters of alfentanil were compared.[7]

Independent verification of CYP3A4 induction: prediction of the effect of efavirenz 600 mg QD on maraviroc, atazanavir and clarithromycin pharmacokinetics

A published maraviroc model [8] was used with one modification: predicted V_{ss} (=1.7 L/kg) versus observed V_{ss} was used in the final model to better recover the observed maraviroc C_{max} following 100 mg twice daily (BID) dosing in healthy volunteers. Ten virtual trials of 12 subjects (age 18-45 years, male only) receiving multiple oral doses of maraviroc (100 mg BID for 14 days), in the presence and absence of efavirenz treatment (600 mg QD for 14 days), were generated and the predicted and observed PK parameters of maraviroc were compared. [9]

Ten virtual trials of 30 subjects receiving a single oral dose of atazanavir (400 mg QD for 20 days), in the presence and absence of efavirenz treatment (600 mg QD on day 7-20), were generated and the predicted and observed PK parameters of atazanavir were compared.[10] Since the age and sex of individuals was not specified an age range of 20 to 50 years and a proportion of females of 0.24 was assumed in the simulation.

Ten virtual trials of 11 subjects receiving oral doses of clarithromycin (500 mg q12h for 7 days), in the presence and absence of efavirenz treatment (400 mg QD for 7 days), were generated and the predicted and observed PK parameters of atazanavir were compared.[10] Since the

age and sex of individuals was not specified an age range of 20 to 50 years and a proportion of females of 0.24 were assumed in the simulation.

Verification of CYP2B6 induction:prediction of the effect of efavirenz 600mg QD on bupropion p.o. pharmacokinetics

Ten virtual trials of 13 subjects (age 21-54 years, female prop. 0.77) receiving a single oral dose of bupropion (150 mg on the morning of day 16), in the presence and absence of efavirenz treatment (600 mg given orally at bedtime for a total of 15 doses), were generated and the predicted and observed plasma concentration-time profiles and PK parameters of bupropion and hydroxybupropion were compared.[11]

Development of efavirenz final model

Simulations assuming fraction absorbed (fa) of 0.67 (1) or fa of 0.4 (2) were compared and fa of 0.67 better recovered the efavirenz systemic exposures following a single dose of 100 to 800 mg. Therefore, the absorption following daily oral dose of efavirenz was described as a first-order process after a lag time (t_{lag} =0.36 h) with f_a of 0.67 and absorption rate constant (k_a) of 0.41 h^{-1}. k_a and t_{lag} were estimated from fitting the observed mean concentration-time profiles following the administration of a single oral dose of 100 mg (unpublished data provided by BMS).

A minimal PBPK model [5] with a single-adjustment compartment (SAC) was fitted to the observed mean concentration-time profiles up to 72 hours following the administration of a single oral dose of 100mg (unpublished data provided by BMS). The SAC compartment lumps all tissues excluding the intestine, liver and portal vein and can be used to represent those organs that make a significant contribution to the volume of distribution. The addition of a SAC compartment was necessary to recover the shape of the plasma concentration-time profiles beyond 24 hours post dosing. The estimated V_{sac} is 1.1 L/kg associated with k_{in} and k_{out} of

0.29 and 0.09 hr-1, respectively. k_{in} and k_{out} are first order rate constants which act on the masses of drug within the systemic compartment and the SAC respectively. All optimization was done using the Weighted Least Square algorithm and Nelder-Mead method.

Although there are *in vitro* data describing the enzyme kinetics for efavirenz in HLMs, [12] [13] these data under-predicted clearance and so were not used in the final model. Instead, input parameters for CL_{int} were back-calculated from observed mean CLpo using the well-stirred liver model, fm for individual CYPs (see below), average population (age-sex matched to the clinical study) values for liver weight (1727 g), microsomal protein per gram of liver (39.0 mg/g) and hepatic CYP enzyme abundance (137,16, 20 and 52 pmol/mg for CYP3A4, 2B6, 2A6 and 1A2, respectively). The observed mean CL_{po} (=5.87 L/hr) [13, 14] following a single dose of 600 mg efavirenz to healthy volunteers was used for the retrograde calculation. CL_{po} from single dose was selected so that the resulting intrinsic clearance could be used in conjunction with the appropriate fm and induction information to predict auto-induction and CL_{po} following multiple dose.

The fm data were derived from HLM data using ticlopidine as an inhibitor of CYP2B6. [13] Although there are rCYP data available, limitations with 2B6 and 2A6 ISEF values will hamper the derivation of an accurate fm. Specifically, in HLM from 7 donors, the formation of 8-OH and 7-OH efavirenz amounted to 77.5% and 22.5% of total metabolite formation. Contribution of CYP2B6 to 8-OH formation (assuming that ticlopidine is specific to CYP2B6) is 81.9% and contribution of CYP2A6 to 7-OH formation is 100%. Other enzymes involved in 8-OH formation include CYP2A6, 1A2, 3A4, 3A5, but the contributions were difficult to quantify. It was, therefore, assumed 2A6, 1A2 and 3A4 contribute equally (~6% each) to 8-OH formation and that CYP3A5 was not expressed in the HLM pool used. Finally, one study reported a role for UGT2B7 [15] but clinical evidence showed this pathway to be negligible. [16] An arbitrary value of 2% of CL_{int} was assigned to additional HLM CL_{int} to represent the UGT2B7 contribution. Therefore, the contribution of CYP2B6, 2A6, 1A2, 3A4 to efavirenz metabolism was assigned

to 62%, 26.6%, 4.6% and 4.6%, respectively. All input parameters are summarized in Table 1.

Verification of final model: prediction of the kinetics of efavirenz following single or multiple oral doses

Ten virtual trials of 10 subjects (aged 20-50 years, male only) receiving a single or multiple oral dose of 400 mg or 600 mg efavirenz for 7 or 10 days were generated and the predicted and observed (400 mg single dose (SD)) [13] and 600 mg QD data were provided by Bristol Myers Squibb (BMS) plasma concentration-time profiles and PK parameters were compared.

Ten virtual trials of 12 subjects (aged 18-40 years, female prop. 0.5) receiving a daily dose of 600 mg efavirenz for 14 days were generated and the predicted and observed plasma concentration-time profiles and PK parameters were compared.[7]

Model development and verification of victim files

Alfentanil model development and verification

Alfentanil model (Supplemental Table 1) was developed based on *in vitro* data and clinical PK data following both i.v. and p.o. administration.[2] fm_{CYP3A4} was set to 93% based on HLM data using ketoconazole or troleandomycin as an inhibitor of CYP3A4.[17] This allowed the recovery of the ketoconazole DDI effect on alfentanil i.v. kinetics: the predicted alfentanil (0.5 mg i.v.) AUC ratio and C_{max} ratio with the co-administration of ketoconazole (400 mg QD for 4 days) were 3.5 (90% CI 3.2-3.7), compared to the observed AUC ratio of 4.8 (90% CI 4.3-5.3).[18] The rest of the metabolism is assigned to additional HLM metabolism (7%). Less than 1% of dose was excreted unchanged in urine. The predicted F_h and F_g are 0.57 and 0.67, consistent with the reported F_h and F_g of 0.58 and 0.71, respectively.

The alfentanil model was subsequently qualified against ketoconazole DDI data (Supplemental Figure 1). The predicted alfentanil (1 mg p.o.) AUC ratio and C_{max} ratio with the co-administration of ketoconazole (400 mg QD for 4 days) were 6.1 (90% CI 5.2-7.1) and 2.6 (90% CI 2.4-2.8), compared to the observed AUC ratio of 9.2 (90% CI 8.0-10.7) and C_{max} ratio of 2.8 (90% not available).[18] The model predictions were within 1.5-fold of the observed values. The discrepancy between the predicted and observed alfentanil AUC ratio may be partly because the dose staggering between ketoconazole and alfentanil dosing was not clearly defined in the study and the simulation assumed a 12-hr dose staggering.[18]

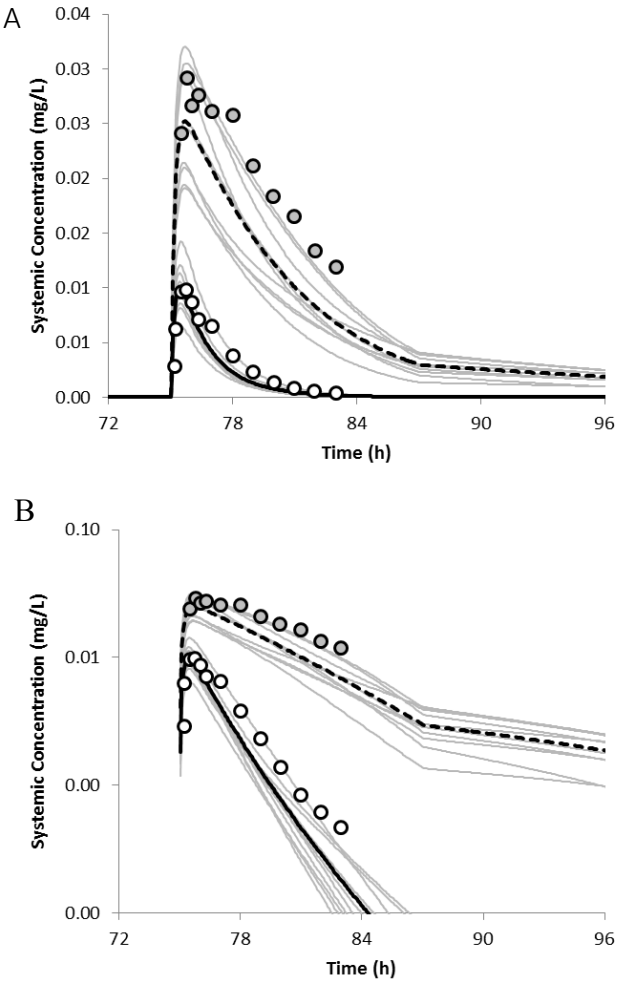

Supplemental Fig. 1. Simulated mean and observed mean plasma concentrations of alfentanil on day 4 following a single oral dose of 1 mg in the absence (solid black line) and presence (dashed line) of ketoconazole treatment (400 mg QD for 3 days) in healthy volunteers

represented on a linear (A) and logarithmic scale (B).[18] The grey lines are the individual trials (10 trials of 6 subjects).

Maraviroc model verification

To verify a published maraviroc model,[8] the effect of ketoconazole treatment (400 mg QD for 9 days) on maraviroc (100 mg BID for 7 days) was simulated based on the study of Abel et al., 2008.[19] The predicted maraviroc AUC ratio was 4.29 (90% CI 4.04-4.55) and C_{max} ratio was 3.22 (90% CI 3.07-3.39), compared to the observed AUC ratio of 5.01 (90% CI 3.98-6.29) and C_{max} ratio of 3.38 (90% CI 2.38-4.78) (Supplemental Figure 2). The model predictions were within 1.2-fold of the observed values.

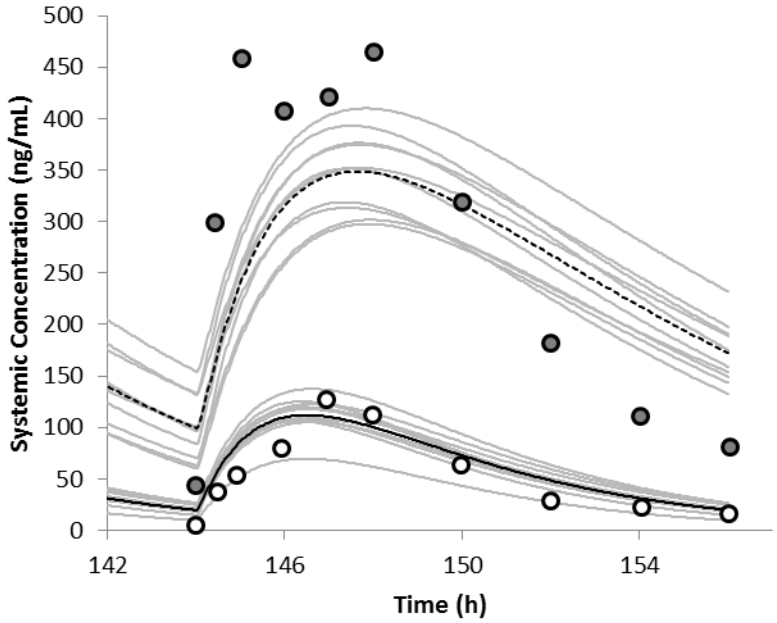

Supplemental Fig. 2. Simulated mean and observed mean plasma concentrations of maraviroc on day 7 following 100 mg BID for 7 days in the absence (solid black line) and presence (dashed line) of ketoconazole treatment (400 mg QD for 9 days) in healthy volunteers.[9] The grey lines are the individual trials (10 trials of 12 subjects).

Atazanavir model development and verification

Atazanavir model (Supplemental Table 2) was developed based on *in vitro* data and clinical PK data following p.o. administration. An atazanavir intrinsic metabolic clearance value of 139.8 µL/min/mg obtained using human liver microsomes has been reported. [20] Data were corrected for nonspecific binding (measured fu_{mic} value corrected for relevant protein concentration was 0.77). Around 7% of an oral dose of atazanavir is excreted unchanged in the urine (CDER Clinical Pharmacology and Biopharmaceutics Review). Thus, a small renal clearance component (0.99 L/h) was also included.[21] A summary of the atazanavir CYP and UGT *in vitro* interaction parameters is also provided in Supplemental Table 2.

To simulate plasma concentration-time profiles of atazanavir after multiple dose administration, the trial design used was based on the studies of McCance-Katz *et al.* 2007.[22] In the McCance-Katz study, ten healthy subjects (26 – 58 years; 4 female; 8 African American, 2 Caucasian) received oral doses of 400 mg atazanavir once daily for 5 days. Since the majority of individuals in the study were African American the CYP3A5 PM phenotype frequency was set to 0.45 and the average hepatic and gut CYP3A5 abundances were reduced to 78 pmol/mg and 18.6 nmol, respectively. Modifications to the CYP3A5 phenotype frequency and abundance were based on the observation of lower incidence of CYP3A5 poor metabolisers and lower CYP3A5 abundance in African Americans compared to Caucasians reported by Kuehl *et al.* 2001.[23]

The atazanavir model incorporating *in vitro* metabolism and CYP and UGT *in vitro* interaction parameters, was verified to ensure the recovery of the non-linear pharmacokinetics following multiple-dose administration (400 mg QD for 5 days) (Supplemental Figure 3). Mean predicted atazanavir C_{max} and AUC values are 3985 ng/mL and 29334 ng/mL*h, respectively, and the corresponding mean observed values are 4435 ng/mL and 29863 ng/mL*h.[22] Dosing of atazanavir alone results in significant inactivation of CYP3A enzymes in both the liver and the gut (data not shown).

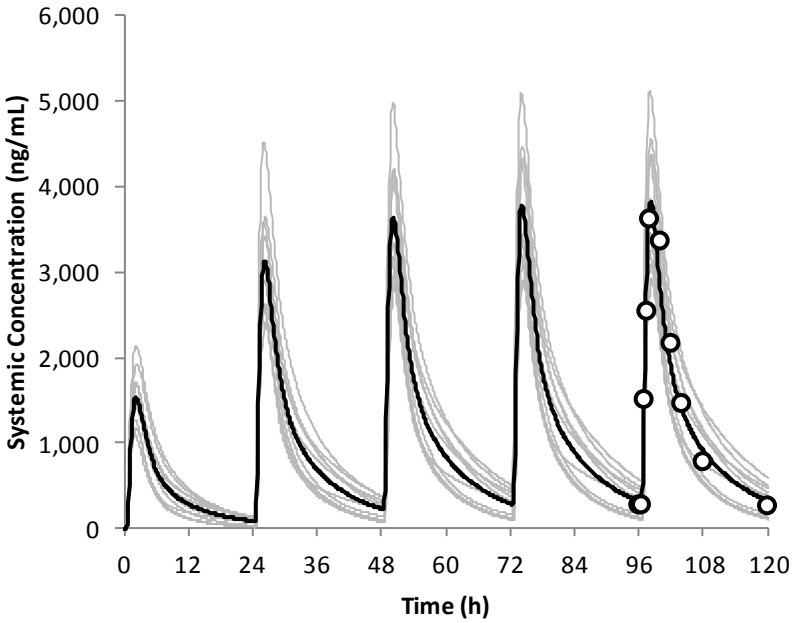

Supplemental Fig 3. Simulated (lines) and observed plasma concentration-time profiles of atazanavir after multiple oral doses of 400 mg to healthy subjects.[22] The grey lines represent individual trials (10 trials of 10 subjects).

Atazanavir model was subsequently qualified against ketoconazole DDI data, based on the study of O'Mara *et al.* 2000.[24] Fifteen healthy subjects received oral doses of 400 mg atazanavir once daily for 13 days. Ketoconazole at 200 mg *QD* was added on Day 7. Since the age and sex of individuals was not specified an age range of 20 to 50 years and proportion of females of 0.24 was assumed in the simulation. Model predicted that co-administration of the potent CYP3A inhibitor ketoconazole (200 mg QD) exerts modest effect on plasma levels of atazanavir. The predicted AUC ratio is 1.31-fold (trial range: 1.16 to 1.53), which is consistent with the observed negligible DDI effect of 1.1-fold. Observed atazanavir plasma concentrations were not available for comparison with model predictions.

Bupropion model development

A model for bupropion sustained release formulation and its major metabolite hydroxybupropion was developed based on *in vitro* data and clinical PK data following p.o. administration (Supplemental Table 3). Bupropion is converted to hydroxybupropion via CYP2B6 and the rest of the metabolism is assigned to additional HLM metabolism. 0.5% of dose is excreted unchanged in urine. fm_{CYP2B6} was set to 58% based on the recovery of observed bupropion and hydroxybupropion plasma concentration-time profiles following a single oral dose of 150 mg based on the study of Loboz *et al.* 2006 (Supplemental Figure 4).[25]

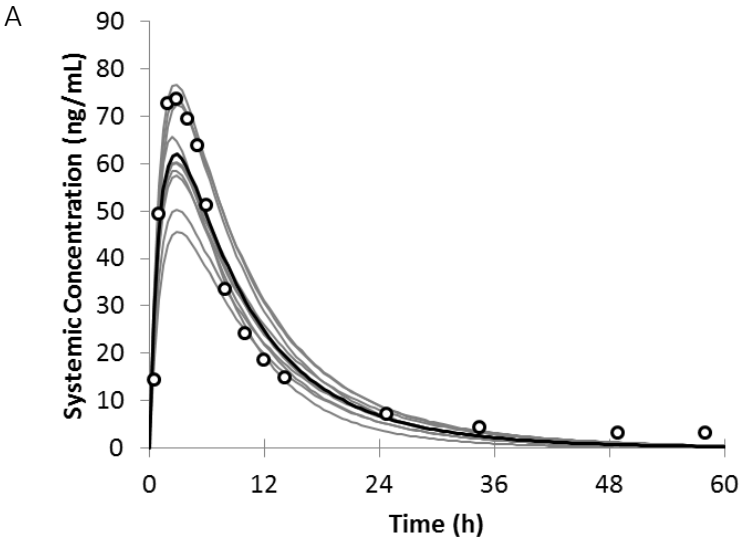

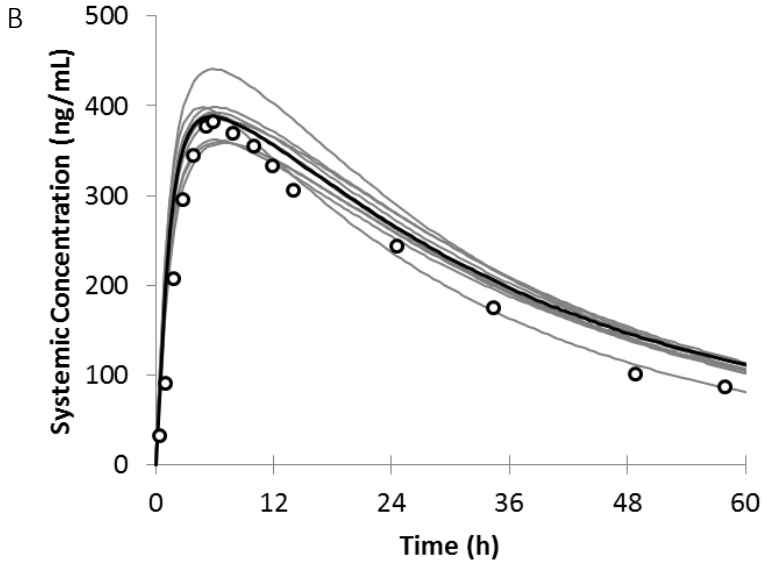

Supplemental Fig. 4. Simulated mean and observed mean plasma concentrations of bupropion (A) and hydroxybupropion (B) following a single oral dose of 150 mg in healthy volunteers.[25] The grey lines are the individual trials (10 trials of 9 subjects).

The predicted geometric mean bupropion C_{max} and AUC values are 57.2 ng/mL and 668 ng/mL*h, respectively, and the corresponding observed values are 63 ng/mL and 696 ng/mL*h.[25] The predicted geometric mean hydroxybupropion C_{max} and AUC values are 351 ng/mL and 14662 ng/mL*h, respectively, and the corresponding observed values are 354 ng/mL and 12700 ng/mL*h.[25] All model predictions were within 1.2-fold of the observed values.

Clarithromycin model verification

Sim-Clarithromycin model was used without modification. Clarithromycin is metabolised by CYP3A4 to two major metabolites 14-(R)-OH clarithromycin and N-demethyl clarithromycin. Enzyme kinetic data generated in a recombinant system were used within the model incorporating Km values for the two routes. [26] Clarithromycin clearance shows nonlinearity with dose due to auto inhibition of CYP3A4, which results in accumulation of clarithromycin after multiple doses. Renal clearance is not dose dependent, with values between 5.8 and 11.9L/h reported in a single ascending dose study of 100 – 1200 mg.[27] Incorporation of both CYP3A4 intrinsic clearance and MBI parameters in the Sim-Clarithromycin model allowed the recovery of clarithromycin exposure following multiple dosing. Predicted and observed Racc mean (range) following the administration of 250 mg BID for 4 days are 1.96 (1.11-4.23) and 1.65 (0.93-3.35), respectively.[28] Ketoconazole DDI data were not available for independent verification of CYP3A4 contribution.

Figure Legends

Supplemental Fig. 1. Simulated mean and observed mean plasma concentrations of alfentanil on day 4 following a single oral dose of 1 mg in the absence (solid black line) and presence (dashed line) of ketoconazole treatment (400 mg QD for 3 days) in healthy volunteers represented on a linear (A) and logarithmic scale (B).[18] The grey lines are the individual trials (10 trials of 6 subjects).

Supplemental Fig. 2. Simulated mean and observed mean plasma concentrations of maraviroc on day 7 following 100 mg BID for 7 days in the absence (solid black line) and presence (dashed line) of ketoconazole treatment (400 mg QD for 9 days) in healthy volunteers.[9] The grey lines are the individual trials (10 trials of 12 subjects).

Supplemental Fig 3. Simulated (lines) and observed plasma concentration-time profiles of atazanavir after multiple oral doses of 400 mg to healthy subjects.[22] The grey lines represent individual trials (10 trials of 10 subjects).

Supplemental Fig. 4. Simulated mean and observed mean plasma concentrations of bupropion (A) and hydroxybupropion (B) following a single oral dose of 150 mg in healthy volunteers.[25] The grey lines are the individual trials (10 trials of 9 subjects).

REFERENCES

1. Poulin P, Haddad S. Advancing prediction of tissue distribution and volume of distribution of highly lipophilic compounds from a simplified tissue-composition-based model as a mechanistic animal alternative method. *J. Pharm. Sci.* 101, 2250-2261 (2012).
2. Almond LM, Mukadam, Iain Gardner, Krystle Okialda, Susan Wong, Oliver Hatley*, et al.* Prediction of DDIs arising from CYP3A induction using a physiologically-based dynamic model. Epub Ahead of Print, (2016).
3. Halladay JS, Wong S, Khojasteh SC, Grepper S. An 'all-inclusive' 96-well cytochrome P450 induction method: measuring enzyme activity, mRNA levels, protein levels, and cytotoxicity from one well using cryopreserved human hepatocytes. *J. Pharmacol. Toxicol. Methods* 66, 270-275 (2012).
4. Almond L, Tay S, Wong S, Mukadam S, Gardner I, Rowland-Yeo K*, et al.* The relationship between mRNA and activity following induction of CYP3A4 and CYP2B6 across a range of prototypical inducers. Poster presented at: 20th North American ISSX Meeting; October 18-22, 2015; Orlando, Florida.
5. Rowland Yeo K, Jamei M, Yang J, Tucker GT, Rostami-Hodjegan A. Physiologically based mechanistic modelling to predict complex drug-drug interactions involving simultaneous competitive and time-dependent enzyme inhibition by parent compound and its metabolite in both liver and gut - the effect of diltiazem on the time-course of exposure to triazolam. *Eur. J. Pharm. Sci.* 39, 298-309 (2010).
6. Ke AB, Nallani SC, Zhao P, Rostami-Hodjegan A, Unadkat JD. Expansion of a PBPK model to predict disposition in pregnant women of drugs cleared via multiple CYP enzymes, including CYP2B6, CYP2C9 and CYP2C19. *Br. J. Clin. Pharmacol.* 77, 554-570 (2014).

7. Kharasch ED, Whittington D, Ensign D, Hoffer C, Bedynek PS, Campbell S*, et al.* Mechanism of efavirenz influence on methadone pharmacokinetics and pharmacodynamics. *Clin. Pharmacol. Ther.* 91, 673-684 (2012).
8. Hyland R, Dickins M, Collins C, Jones H, Jones B. Maraviroc: in vitro assessment of drug-drug interaction potential. *Br. J. Clin. Pharmacol.* 66, 498-507 (2008).
9. Abel S, Jenkins TM, Whitlock LA, Ridgway CE, Muirhead GJ. Effects of CYP3A4 inducers with and without CYP3A4 inhibitors on the pharmacokinetics of maraviroc in healthy volunteers. *Br. J. Clin. Pharmacol.* 65 Suppl 1, 38-46 (2008).
10. FDA, CDER. Sustiva Clinical Pharmacology and Biopharmaceutics Review. (2006). Available From: http://www.accessdata.fda.gov/drugsatfda_docs/nda/98/20972.cfm
11. Robertson SM, Maldarelli F, Natarajan V, Formentini E, Alfaro RM, Penzak SR. Efavirenz induces CYP2B6-mediated hydroxylation of bupropion in healthy subjects. *J. Acquir. Immune Defic. Syndr.* 49, 513-519 (2008).
12. Xu C, Ogburn ET, Guo Y, Desta Z. Effects of the CYP2B6*6 allele on catalytic properties and inhibition of CYP2B6 in vitro: implication for the mechanism of reduced efavirenz metabolism and other CYP2B6 substrates in vivo. *Drug Metab. Dispos.* 40, 717-725 (2012).
13. Ogburn ET, Jones DR, Masters AR, Xu C, Guo Y, Desta Z. Efavirenz primary and secondary metabolism in vitro and in vivo: identification of novel metabolic pathways and cytochrome P450 2A6 as the principal catalyst of efavirenz 7-hydroxylation. *Drug Metab. Dispos.* 38, 1218-1229 (2010).
14. Zhu M, Kaul S, Nandy P, Grasela DM, Pfister M. Model-based approach to characterize efavirenz autoinduction and concurrent enzyme induction with carbamazepine. *Antimicrob. Agents Chemother.* 53, 2346-2353 (2009).
15. Bae SK, Jeong YJ, Lee C, Liu KH. Identification of human UGT isoforms responsible for glucuronidation of efavirenz and its three hydroxy metabolites. *Xenobiotica* 41, 437-444 (2011).

16. Cho DY, Ogburn ET, Jones D, Desta Z. Contribution of N-glucuronidation to efavirenz elimination in vivo in the basal and rifampin-induced metabolism of efavirenz. *Antimicrob. Agents Chemother.* 55, 1504-1509 (2011).

17. Labroo R, Kharasch ED. Gas chromatographic-mass spectrometric analysis of alfentanil metabolites. Application to human liver microsomal alfentanil biotransformation. *J. Chromatogr. B. Biomed. Appl.* 660, 85-94 (1994).

18. Kharasch ED, Vangveravong S, Buck N, London A, Kim T, Blood J*, et al.* Concurrent assessment of hepatic and intestinal cytochrome P450 3A activities using deuterated alfentanil. *Clin. Pharmacol. Ther.* 89, 562-570 (2011).

19. Abel S, Russell D, Taylor-Worth RJ, Ridgway CE, Muirhead GJ. Effects of CYP3A4 inhibitors on the pharmacokinetics of maraviroc in healthy volunteers. *Br. J. Clin. Pharmacol.* 65 Suppl 1, 27-37 (2008).

20. Wempe MF, Anderson PL. Atazanavir metabolism according to CYP3A5 status: an in vitro-in vivo assessment. *Drug Metab. Dispos.* 39, 522-527 (2011).

21. Anderson PL, Aquilante CL, Gardner EM, Predhomme J, McDaneld P, Bushman LR*, et al.* Atazanavir pharmacokinetics in genetically determined CYP3A5 expressors versus non-expressors. *J. Antimicrob. Chemother.* 64, 1071-1079 (2009).

22. McCance-Katz EF, Moody DE, Morse GD, Ma Q, DiFrancesco R, Friedland G*, et al.* Interaction between buprenorphine and atazanavir or atazanavir/ritonavir. *Drug Alcohol Depend.* 91, 269-278 (2007).

23. Kuehl P, Zhang J, Lin Y, Lamba J, Assem M, Schuetz J*, et al.* Sequence diversity in CYP3A promoters and characterization of the genetic basis of polymorphic CYP3A5 expression. *Nat. Genet.* 27, 383-391 (2001).

24. O'Mara E, Randall D, Mummaneni V, Uderman H, Knox L, Schuster A*, et al.* Steady-State Pharmacokinetic Interaction Study between BMS-232632 and Ketoconazole in Healthy Subjects. Poster presented at: 40th Interscience Conference on Antimicrobial Agents and Chemotherapy; September 17-20, 2000; Toronto.

25. Loboz KK, Gross AS, Williams KM, Liauw WS, Day RO, Blievernicht JK*, et al.* Cytochrome P450 2B6 activity as measured by bupropion hydroxylation: effect of induction by rifampin and ethnicity. *Clin. Pharmacol. Ther.* 80, 75-84 (2006).

26. Rodrigues AD, Roberts EM, Mulford DJ, Yao Y, Ouellet D. Oxidative metabolism of clarithromycin in the presence of human liver microsomes. Major role for the cytochrome P4503A (CYP3A) subfamily. *Drug Metab. Dispos.* 25, 623-630 (1997).

27. Chu SY, Sennello LT, Bunnell ST, Varga LL, Wilson DS, Sonders RC. Pharmacokinetics of clarithromycin, a new macrolide, after single ascending oral doses. *Antimicrob. Agents Chemother.* 36, 2447-2453 (1992).

28. Chu S, Wilson DS, Deaton RL, Mackenthun AV, Eason CN, Cavanaugh JH. Single- and multiple-dose pharmacokinetics of clarithromycin, a new macrolide antimicrobial. *J. Clin. Pharmacol.* 33, 719-726 (1993).

29. Meuldermans WE, Hurkmans RM, Heykants JJ. Plasma protein binding and distribution of fentanyl, sufentanil, alfentanil and lofentanil in blood. *Arch. Int. Pharmacodyn. Ther.* 257, 4-19 (1982).

30. Bower S, Hull CJ. Comparative pharmacokinetics of fentanyl and alfentanil. *Br. J. Anaesth.* 54, 871-877 (1982).

31. Meistelman C, Saint-Maurice C, Lepaul M, Levron JC, Loose JP, Mac Gee K. A comparison of alfentanil pharmacokinetics in children and adults. *Anesthesiology* 66, 13-16 (1987).

32. Schuttler J, Stoeckel H. [Clinical pharmacokinetics of alfentanyl (author's transl)]. *Anaesthesist* 31, 10-14 (1982).

33. Beaumont K, Gardner I, Chapman K, Hall M, Rowland M. Toward an integrated human clearance prediction strategy that minimizes animal use. *J. Pharm. Sci.* 100, 4518-4535 (2011).

34. Roure P, Jean N, Leclerc AC, Cabanel N, Levron JC, Duvaldestin P. Pharmacokinetics of alfentanil in children undergoing surgery. *Br. J. Anaesth.* 59, 1437-1440 (1987).

35. Mather LE. Clinical pharmacokinetics of fentanyl and its newer derivatives. *Clin. Pharmacokinet.* 8, 422-446 (1983).

36. Gertz M, Harrison A, Houston JB, Galetin A. Prediction of human intestinal first-pass metabolism of 25 CYP3A substrates from in vitro clearance and permeability data. *Drug Metab. Dispos.* 38, 1147-1158 (2010).

37. Kharasch ED, Bedynek PS, Hoffer C, Walker A, Whittington D. Lack of indinavir effects on methadone disposition despite inhibition of hepatic and intestinal cytochrome P4503A (CYP3A). *Anesthesiology* 116, 432-447 (2012).

38. Kharasch ED, Bedynek PS, Walker A, Whittington D, Hoffer C. Mechanism of ritonavir changes in methadone pharmacokinetics and pharmacodynamics: II. Ritonavir effects on CYP3A and P-glycoprotein activities. *Clin. Pharmacol. Ther.* 84, 506-512 (2008).

39. Kharasch ED, Francis A, London A, Frey K, Kim T, Blood J. Sensitivity of intravenous and oral alfentanil and pupillary miosis as minimal and noninvasive probes for hepatic and first-pass CYP3A induction. *Clin. Pharmacol. Ther.* 90, 100-108 (2011).

40. Kharasch ED, Hoffer C, Whittington D, Walker A, Bedynek PS. Methadone pharmacokinetics are independent of cytochrome P4503A (CYP3A) activity and gastrointestinal drug transport: insights from methadone interactions with ritonavir/indinavir. *Anesthesiology* 110, 660-672 (2009).

41. Kharasch ED, Stubbert K. Cytochrome P4503A does not mediate the interaction between methadone and ritonavir-lopinavir. *Drug Metab. Dispos.* 41, 2166-2174 (2013).

42. Kharasch ED, Walker A, Hoffer C, Sheffels P. Intravenous and oral alfentanil as in vivo probes for hepatic and first-pass cytochrome P450 3A activity: noninvasive assessment by use of pupillary miosis. *Clin. Pharmacol. Ther.* 76, 452-466 (2004).

43. Kharasch ED, Walker A, Hoffer C, Sheffels P. Sensitivity of intravenous and oral alfentanil and pupillary miosis as minimally invasive and noninvasive probes for hepatic and first-pass CYP3A activity. *J. Clin. Pharmacol.* 45, 1187-1197 (2005).

44. Kharasch ED, Walker A, Isoherranen N, Hoffer C, Sheffels P, Thummel K*, et al.* Influence of CYP3A5 genotype on the pharmacokinetics and pharmacodynamics of the cytochrome P4503A probes alfentanil and midazolam. *Clin. Pharmacol. Ther.* 82, 410-426 (2007).

45. Rodgers T, Rowland M. Mechanistic approaches to volume of distribution predictions: understanding the processes. *Pharm. Res.* 24, 918-933 (2007).

46. Meuldermans W, Van Peer A, Hendrickx J, Woestenborghs R, Lauwers W, Heykants J*, et al.* Alfentanil pharmacokinetics and metabolism in humans. *Anesthesiology* 69, 527-534 (1988).

47. FDA, CDER. Atazanavir Clinical Pharmacology and Biopharmaceutics Review. (2002). Available From: http://www.accessdata.fda.gov/drugsatfda_docs/nda/2003/21-567_Reyataz_BioPharmr_P1.pdf

48. Goldsmith DR, Perry CM. Atazanavir. *Drugs* 63, 1679-1693; discussion 1694-1675 (2003).

49. Lepist EI, Phan TK, Roy A, Tong L, Maclennan K, Murray B*, et al.* Cobicistat boosts the intestinal absorption of transport substrates, including HIV protease inhibitors and GS-7340, in vitro. *Antimicrob. Agents Chemother.* 56, 5409-5413 (2012).

50. Bristol-Myers Squibb Company. Reyataz (Atazanavir) Prescribing Information. (2015). Available From: http://www.accessdata.fda.gov/drugsatfda_docs/label/2015/206352s003,021567s038lbl.pdf

51. Findlay JW, Van Wyck Fleet J, Smith PG, Butz RF, Hinton ML, Blum MR*, et al.* Pharmacokinetics of bupropion, a novel antidepressant agent, following oral administration to healthy subjects. *Eur. J. Clin. Pharmacol.* 21, 127-135 (1981).

52. Poulin P, Theil FP. Prediction of pharmacokinetics prior to in vivo studies. 1. Mechanism-based prediction of volume of distribution. *J. Pharm. Sci.* 91, 129-156 (2002).

53. Posner J, Bye A, Dean K, Peck AW, Whiteman PD. The disposition of bupropion and its metabolites in healthy male volunteers after single and multiple doses. *Eur. J. Clin. Pharmacol.* 29, 97-103 (1985).

54. Palovaara S, Pelkonen O, Uusitalo J, Lundgren S, Laine K. Inhibition of cytochrome P450 2B6 activity by hormone replacement therapy and oral contraceptive as measured by bupropion hydroxylation. *Clin. Pharmacol. Ther.* 74, 326-333 (2003).

55. Kustra R, Corrigan B, Dunn J, Duncan B, Hsyu PH. Lack of effect of cimetidine on the pharmacokinetics of sustained-release bupropion. *J. Clin. Pharmacol.* 39, 1184-1188 (1999).

Supplemental Table 1 – Input parameters of alfentanil

Parameter	Value	Reference
Molecular weight	416.52	
fu	0.12	Meta-analysis [29] [30-32] [33, 34]
B:P	0.66	[29, 33]
logP	2.16	[35]
Compound type	Monoprotic Base	
pKa(s)	6.5	[29, 35]
fa – predicted	0.99	Predicted from Caco-2 data [36]
ka (h^{-1}) - predicted	4.8	Predicted from Caco-2 data [36]
Qgut (L/h)	2.2	Optimised to recover observed F_G. [18, 37-44]
Caco-2 (Papp A-B)	293	[36]
fu_{gut}	1	Assumed
V_{ss}(L/kg) – predicted (Minimal PBPK)	0.397	Rodgers and Rowland method [45]
V_{ss} (L/kg) - observed	0.371	Meta-analysis [2]
CL_{iv} (L/h)	19.9	Meta-analysis [2]
rCYP3A4 CL_{int} (µL/min/pmol)	0.49	Calculated from CL_{iv} using the Retrograde model and fm_{CYP3A4} = 0.93
Add CL_{int} (µL/min/mg mic protein)	4.37	Calculated using the Retrograde model
CL_R (L/h)	0.06	Meta-analysis [32, 46]

Supplemental Table 2 – Input parameters of Atazanavir

Parameter	Atazanavir	Source
Molecular weight	705	
Log P	4.5	Calculated– Drug Bank
Compound type	Monoprotic Base	[47]
pKa	5.62	[47]
B:P ratio	0.75	[8]
Fu	0.14	[24]
Main plasma binding protein	AGP	[48]
P_{app} Caco-2 pH 7.4:7.4 (x 10^{-6} cm/s)	19.12[#]	[49]
P_{eff},man (10^{-4} cm/s)	2.11	
fa	0.91	predicted from P_{eff},man
ka (h^{-1})	0.87	predicted from P_{eff},man
Lag time (h)	1.0	Applied to recover observed t_{max}
Q_{gut} (L/h)	9.3	predicted from P_{eff},man (predicted from Caco-2)
fugut	0.14	Equal to fu
V_{ss} (L/kg)	1.12	Fitted to observed V/F data following correction for F
Lag time (h)	1.0	Applied to recover observed tmax
CYP3A4 CL_{int} (µl/min/pmol)	1.19	Calculated from HLM CL_{int} based on average CYP3A4 abundance (137 pmol/mg) and *in vitro* fm 0.9
CYP3A5 CL_{int} (µl/min/pmol)	1.19	Assuming CYP3A5 CL_{int} per unit enzyme that is equal to CYP3A4
Non-3A CL_{int} (µl/min/mg)	18	Calculated from HLM CL_{int} based *in vitro* fm 0.1
CYP2C8 Ki (µM)	2.1	[47]
CYP1A2 Ki (µM)	12.1	[47]
CYP2C19 Ki (µM)	12.7	[47]

CYP3A4 Ki (µM)	2.35	[47]
UGT1A1 Ki (µM)	1.9	[47]
CYP3A4/5 K_I (µM)	0.84	[50] Assumed to inhibit CYP3A5 with the same potency as CYP3A4.
CYP3A4/5 K_{inact} (h^{-1})	3	[50]

Supplemental Table 3 – Input parameters of bupropion and hydroxybupropion

Parameter	Value	Reference
Bupropion		
MW	239.74	
fu	0.16	[51]
B:P	0.82	Personal Communication
logP	3.4	Personal Communication
Compound type	Monoprotic Base	
pKa(s)	8.02	Marvin (ChemAxon)
fa – user input	1	
ka (h^{-1}) - optimised	0.82	Optimised parameter
Qgut (L/h)	14.6	Predicted from physchem
PSA (A^2)	29.1	Marvin (ChemAxon)
HBD	1	Marvin (ChemAxon)
fu_{gut}	1	
V_{ss}(L/kg) (Minimal PBPK)	5.8	Optimized; Predicted value is 4.8 L/kg using Rodgers and Rowland method[45]
Oral Clearance (L/h)	200	Meta-analysis
rCYP2B6 CL_{int} (µL/min/pmol)	12.2	Calculated from CL_{PO} using the Retrograde model and fm_{2B6} = 0.58
Add CL_{int} (µL/min/mg mic protein)	126	Calculated using the Retrograde model
CL_R (L/h)	0.46	
OH-Bupropion		
MW	255.74	
fu	0.16*	
B:P	0.82*	
logP	2.9	AlogPS; ChemAxon (via Drugbank)
Compound type	Monoprotic Base	
pKa(s)	8.02	ChemAxon (via Drugbank)
V_{ss}(L/kg) (Minimal PBPK)	2.1	Predicted using Poulin and Theil method [52]
In vivo oral clearance (L/h)	4.9	Calculated from *in vivo* elimination rate constant [25, 38, 53-55] and V_{ss}

*Bupropion value assumed due to a lack of specific information for OH-bupropion